Chinese Chemical Letters 37 (2026) 111095

Contents lists available at ScienceDirect

Chinese Chemical Letters

journal homepage: www.elsevier.com/locate/cclet

Electron transfer chemistry triggered by silicon-doped carbon catalysts derived from natural minerals for the degradation of organic pollutants

Wan-Yin Gao[a,b], Xiao-Qiang Cao[a,b,*], Li-Fei Hou[a,b], Hao-Yun Lu[a,b], Zhao-Jing Zhu[d], Wen-Jia Kong[e], Yang Zhang[a,b], Yi-Zhen Zhang[a,b], Ya-Nan Shang[a,b,*], Xing Xu[c]

[a] College of Safety and Environmental Engineering, Shandong University of Science and Technology, Qingdao 266590, China
[b] Institute of Yellow River Delta Earth Surface Processes and Ecological Integrity, Shandong University of Science and Technology, Qingdao 266590, China
[c] Shandong Key Laboratory of Water Pollution Control and Resource Reuse, School of Environmental Science and Engineering, Shandong University, Qingdao 266237, China
[d] Qingdao Ecology and Environment Bureau, West Coast New Area Branch, Qingdao 266555, China
[e] College of Resources and Environment, Key Laboratory of Agricultural Environment, Shandong Agricultural University, Tai'an 271000, China

ARTICLE INFO

Article history:
Received 22 November 2024
Revised 20 January 2025
Accepted 15 March 2025
Available online 16 March 2025

Keywords:
Peroxymonosulfate
Electron transfer process
Antibiotics
Organic pollutants
Fenton-like reaction
Montmorillonite

ABSTRACT

In this study, we meticulously designed a layered carbon-based catalytic material to induce the degradation of a series of organic pollutants by activating peroxymonosulfate (PMS) in the PMS-based advanced oxidation processes (AOPs). Results indicated that the silicon and oxygen elements from the montmorillonite were incorporated into the catalyst matrix to form the Si-O-C structure. It was notable that the layered carbonaceous material with Si-O-C structure exhibited an outstanding catalytic effect on the synthesized layered catalytic material array, achieving over 90% removal rate of most pollutants within 60 min. It was notable that the layered carbonaceous material with Si-O-C structure exhibited an outstanding catalytic effect on the synthesized layered catalytic material array. The salt bridge system confirmed that pollutants can provide electrons to the Si-O-C/PMS system, and we verified that the electron transfer process (ETP) mechanism was the main pathway for the degradation of pollutants in the Si-O-C/PMS system *via* the open-circuit potential analysis. In combination with the structural properties of different pollutants, we discovered that electron-donating pollutants can supply more electrons to the Si-O-C/PMS system, thereby enhancing the ETP process. The findings of this study are anticipated to advance the development and practical application of layered carbonaceous materials-based catalysts and support the design and implementation of nanoconfined catalysts in the field of AOPs.

© 2025 Published by Elsevier B.V. on behalf of Chinese Chemical Society and Institute of Materia Medica, Chinese Academy of Medical Sciences.

New pollutants refer to toxic and harmful chemicals that possess characteristics such as biological toxicity, environmental persistence, and bioaccumulation. Once they enter the environment, they pose significant risks to the ecological environment or human health. Yet they have not been incorporated into environmental management or existing management measures are insufficient. Usually, new pollutants that have gained widespread attention mainly fall into four categories: Persistent organic pollutants, endocrine-disrupting chemicals, antibiotics, and microplastics [1,2]. Of these new pollutants, the production and use of antibiotics is mostly huge because of their proximity to our daily lives. However, only a portion of the antibiotics are effectively absorbed and metabolized. The majority of the residues are discharged, either directly or indirectly, into the natural aquatic environment. Despite the low toxicity of antibiotics, they can rapidly accumulate through various pathways, generate resistance genes, and pose risks to the environment and human health [3,4].

In recent years, the advanced oxidation process (AOPs) based on heterogeneous peroxymonosulfate has been widely applied in the research of organic wastewater treatment due to its high oxidative capacity, rapid reaction kinetics, and broadly applicable pH range [5]. Currently, numerous scholars have developed a variety of strategies to activate peroxymonosulfate (PMS) by introducing additional energy sources (such as thermal treatment, ultraviolet irradiation, and ultrasonic assistance) and materials like transition metals and carbon-based materials [6–8]. These strategies aim to generate reactive species (ROSs) to oxidize and remove pollutants [9–11]. The generation of reactive oxygen species (ROS) differs sig-

* Corresponding authors.
E-mail addresses: caoxiaoqiang@sdust.edu.cn (X.-Q. Cao), shangyanan@sdust.edu.cn (Y.-N. Shang).

https://doi.org/10.1016/j.cclet.2025.111095
1001-8417/© 2025 Published by Elsevier B.V. on behalf of Chinese Chemical Society and Institute of Materia Medica, Chinese Academy of Medical Sciences.

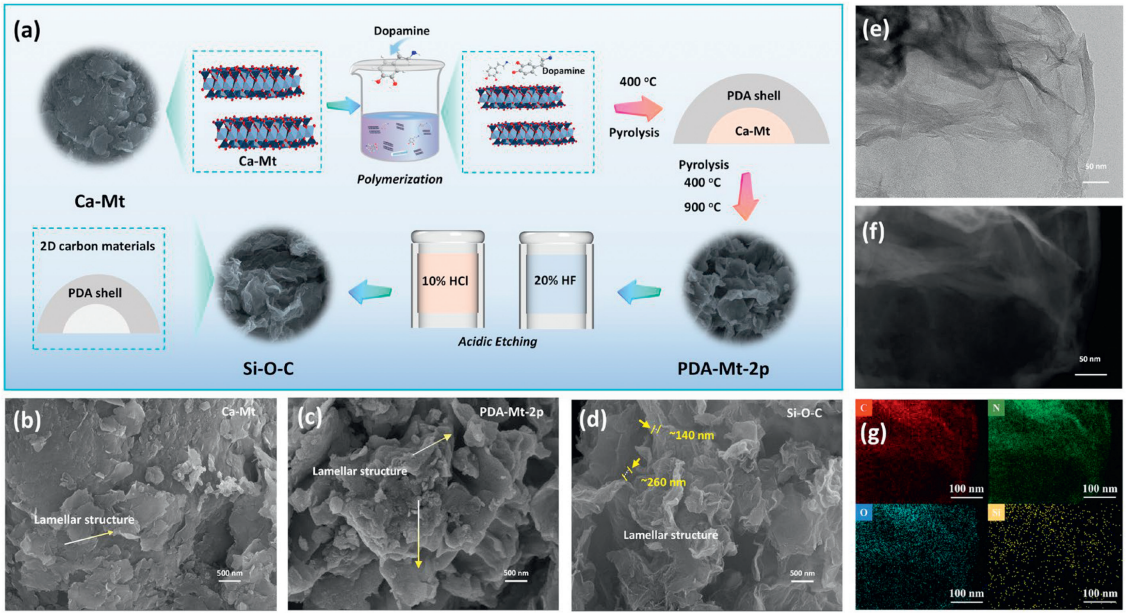


Fig. 1. (a) The preparation process of PDA-Mt-2p and Si-O-C. SEM image of (b) Ca-Mt, (c) PDA-Mt-2p, (d) Si-O-C. (e) TEM of Si-O-C. (f) HAADF-STEM of Si-O-C. (g) TEM mappings of Si-O-C.

nificantly among various advanced oxidation process (AOP) systems, leading to variations in the degradation efficiency of pollutants. Additionally, organic pollutants constitute a large category of pollutants, each with distinct properties. However, current research primarily focuses on the degradation of a specific one using a particular AOP system. Therefore, it is increasingly important to develop AOP systems which can be used in degradation of various organic pollutants.

Transition metals such as cobalt (Co), manganese (Mn), and iron (Fe) have shown significant effectiveness in the activation of PMS for the degradation of pollutants [12,13]. However, metal catalysts pose the risk of metal leaching, leading to secondary pollution. Dopamine is a widely used chemical in environmental functional materials, which can self-polymerize under alkaline environmental conditions and firmly adhere to various substrates to form conformal coatings [14]. A dopamine-triggered encapsulation strategy had been designed in previous studies, resulting in a thin carbon layer of polydopamine coated on silicon nanospheres [15]. However, these nitrogen-containing carbon materials, such as dopamine (DA) monomers, tend to aggregate due to initial polymerization, which may obscure the internal reactive sites and reduce their catalytic activity. A feasible solution is *in situ* polymerization on one- or two-dimensional nanosubstrates, which can reduce the agglomeration of nanoparticles and can enhance the mass transfer of ROS by spatially limiting the domains, thus improving the degradation efficiency of pollutants [16]. Two-dimensional (2D) layered montmorillonite are considered to be ideal heterogeneous metal-free template because of their expandable interlayer domain and a layered structure, a unique pore structure, good mechanical strength, and stable tetrahedral siloxane and octahedral alumoxane structures which can provide abundant catalytic sites and high specific surface area [17,18]. Montmorillonite can not only be used as an adsorbent and catalyst support in the field of environmental remediation [19,20], but also considered an ideal template for the *in-situ* transformation of organic matter in the surface and interlayer domains into two-dimensional carbon materials.

Therefore, in this study, montmorillonite was utilized as a catalyst carrier by capitalizing on the inherent advantages of natural clay minerals (Fig. 1a). Through the *in-situ* polymerization of dopamine on calcium montmorillonite (Ca-Mt), more active centers were generated in Ca-Mt. Hence, the montmorillonite-derived carbon material with a Si-O-C structure synthesized by this approach would significantly enhance its Fenton-like catalytic activity. On this basis, the oxidation characteristics of the Si-O-C catalyst towards a series of antibiotic pollutants and its possible degradation patterns were determined by the PMS activation system.

The scanning electron microscopy (SEM) images, as presented in Figs. 1b-d, revealed that the Ca-Mt exhibited a lamellar configuration characterized by a uniformly smooth and compact surface morphology. In contrast, the PDA-Mt-2p was distinguished by a rugged and porous surface topography, a feature that was attributed to the pyrolytic decomposition of the PDA shell. The Si-O-C catalyst was typified by a curled, lamellar fold structure, and it was noteworthy that the catalyst retained the intrinsic lamellar characteristics of the montmorillonite even after hydrofluoric acid (HF) etching. Further corroboration of the layered structure of Si-O-C was provided by the transmission electron microscopy (TEM) images presented in Figs. 1e-g. Additionally, various elements (Si, C, N, O) were uniformly distributed across the catalyst surface with a high C content (>87 %). This observation suggested that the catalyst underwent a transformation into a carbonaceous material through the processes of pyrolysis and etching. Furthermore, the incorporation of silicon and oxygen elements from the montmorillonite into the catalyst matrix was evidenced by their uniform distribution, indicating a successful doping process that may enhance the material's catalytic properties.

The N_2 adsorption-desorption isotherm of Ca-Mt (Fig. 2a) exhibited a Type IV curve with an H3 hysteresis loop, indicating the presence of narrow slit-like pore structures within the sample, which are formed by the aggregation of fine particles [21]. After pyrolysis, the adsorption capacity of PDA-Mt-2p was significantly enhanced, which was attributed to the high-temperature pyrolysis of PDA in the interlayer and on the surface of montmorillonite, resulting in the formation of a porous structure and a larger specific surface area. However, when subjected to excessively high temperatures, montmorillonite might undergo structural collapse and sintering. The BET surface areas as well as pore volumes of Si-O-C and Ca-Mt were similar (Fig. 2a and Table S1 in Supporting information), which further confirmed that Si-O-C had a montmorillonite-like configuration. As shown in Fig. 2b, it was evident that the pore

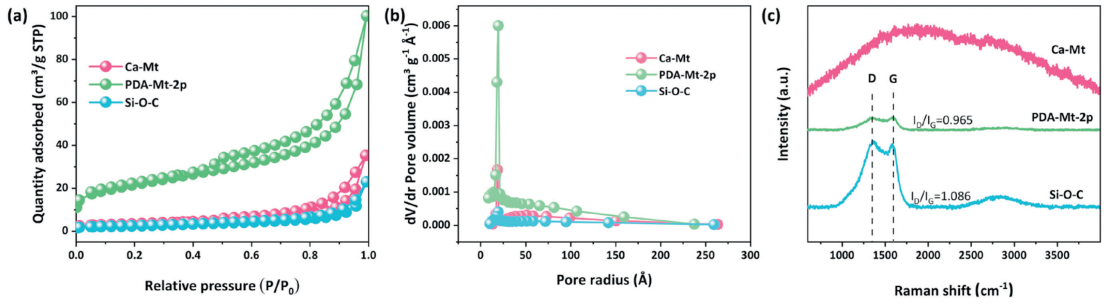


Fig. 2. (a) N_2 adsorption–desorption isotherms, (b) pore size distribution and (c) Raman spectra of Ca-Mt, PDA-Mt-2p and Si-O-C.

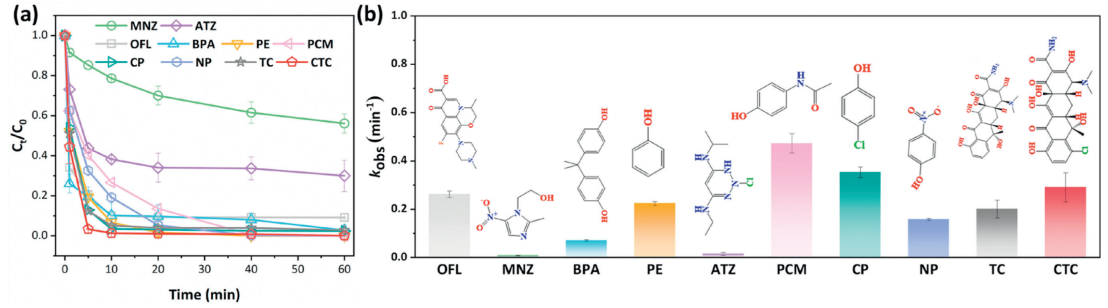


Fig. 3. (a) Degradation of different contaminants in the Si-O-C/PMS system with 2.0 mmol/L PMS. (b) The k_{obs} of different contaminants degradation. Catalyst dosage: 0.1 g/L; PMS dosage: 2.0 mmol/L; Pollutant concentration: 10 mg/L.

size distribution of each sample predominantly centered around 19 Å, indicating a mesoporous structure as the primary characteristic of the catalyst. Further examination of the structural configuration of the catalyst can be observed from the Raman spectra (Fig. 2c). The intensity ratio of the D band (1360 cm^{-1}) to the G band (1600 cm^{-1}), denoted as I_D/I_G, was an important parameter that could reflect the defect sites/graphitic structure of carbonaceous materials [22,23]. The I_D/I_G value of PDA-Mt-2p was calculated to be 0.965, indicating that the calcination process could promote the formation of a graphitic carbon structure on montmorillonite. After etching, the I_D/I_G ratio increases from 0.965 to 1.086, suggesting that the as-prepared Si-O-C catalyst had a more defective structure, which might provide more active sites for the activation of PMS in the Si-O-C/PMS system [24].

The degradation performance of Ca-Mt, PDA-Mt-2p and Si-O-C was presented in Fig. S1 (Supporting information), which showed that the Si-O-C has obvious superiority in degradation of ofloxacin (OFL) than Ca-Mt, PDA-Mt-2p. A variety of organic pollutants, including metronidazole (MNZ), bisphenol A (BPA), phenol (PE), atrazine (ATZ), paracetamol (PCM), 4-chlorophenol (CP), nitrophenol (NP), tetracycline (TC), and chlortetracycline (CTC), were selected as target contaminants to further evaluate the catalytic performances of the Si-O-C/PMS system, as depicted in Fig. 3a. The results indicated that the majority of these pollutants were removed by >90% within a 60-min timeframe, with the exception of MNZ and ATZ, which exhibited less satisfactory removal efficiencies. The Si-O-C/PMS system demonstrated a commendable catalytic degradation capability for certain recalcitrant organic pollutants. The k_{obs} of the Si-O-C/PMS systems for different pollutants were significantly different in the range of 0.1647–0.2648 min^{-1} (Fig. 3b), suggesting that the catalytic degradation pathway might be correlated with the pollutant species [25].

To further investigate the degradation behavior of various pollutant in Si-O-C/PMS system, the degradation of recalcitrant pollutants, exemplified by MNZ, BPA, PE, and ATZ, was conducted under varying doses of PMS as depicted in Figs. 4a-d. The concentrations of the organic compounds were quantified using high-performance liquid chromatography (HPLC). The detailed detection conditions are provided in Table S2 (Supporting information). The catalytic efficacy of the Si-O-C in the degradation of these pollutants was observed to be markedly distinct with the escalation of the PMS dosage. Notably, the degradation rates of MNZ and ATZ were substantially enhanced within the Si-O-C/PMS system, as illustrated in Figs. 4a and b. When the PMS concentration was elevated from 0.5 mmol/L to 3.3 mmol/L, the observed k_{obs} for MNZ and ATZ increased dramatically, from 0.0016 min^{-1} to 0.0257 min^{-1} and from 0.0026 min^{-1} to 0.0188 min^{-1}, respectively, representing an approximately 16-fold and 7-fold increase (Fig. 4e). These findings suggested that oxidative capacity of the Si-O-C towards MNZ and ATZ was highly responsive to the PMS dosage, achieving a significant removal efficiency at elevated PMS levels. In contrast to MNZ and ATZ, BPA and PE demonstrated rapid degradation kinetics even at the lowest PMS dose of 0.5 mmol/L, with corresponding k_{obs} values of 0.0707 and 0.1647 min^{-1}, as shown in Fig. 4e. The distinct catalytic behaviors of Si-O-C in degrading the four pollutants give rise to the hypothesis that multiple oxidation pathways might be in operation within the catalytic system. Furthermore, it was proposed that the predominant oxidation pathway was susceptible to the specific features of the target pollutants, which could account for the observed variations in degradation kinetics.

To substantiate the occurrence of electron transfer within the Si-O-C/PMS matrix, methodologies involving the measurement of open circuit potential (OCP) and the establishment of a galvanic oxidation system (GOS) were meticulously executed. As shown in Fig. 5a, OCP dynamic measurements demonstrate the presence of electron transfer in the Si-O-C/PMS system. Upon the introduction of PMS at 120 s, a pronounced elevation in potential was observed, signifying the complexation of Si-O-C with PMS and concomitant augmentation of its oxidative potential. This potential alteration became progressively pronounced with an incremental dose of PMS. As depicted in Fig. S2 (Supporting information), the Si-O-C/PMS system exhibited a markedly greater potential shift (increasing from 0.069 eV to 0.0092 eV) compared to the Ca-Mt/PMS

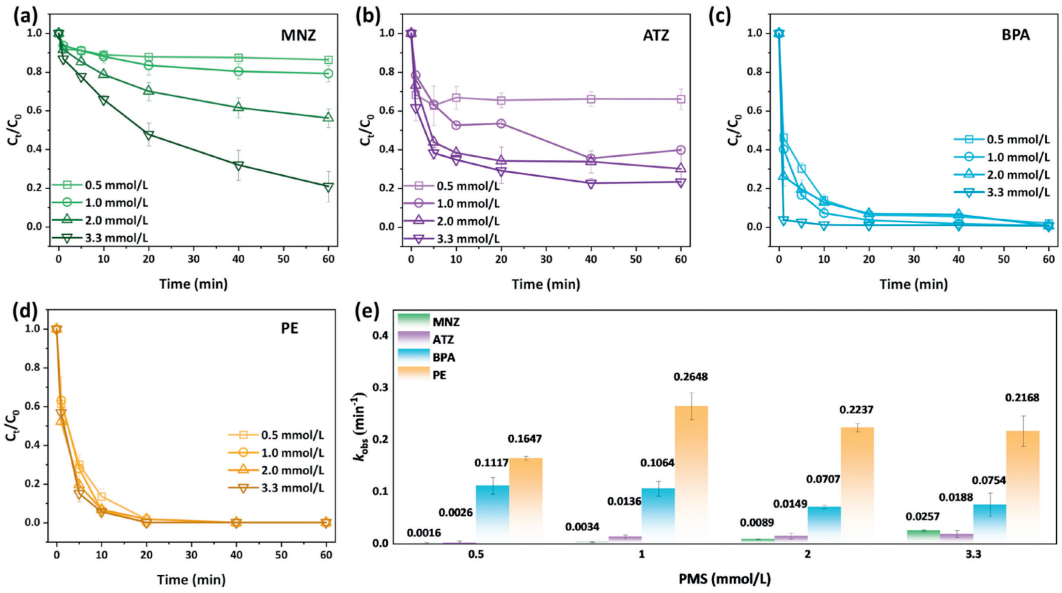


Fig. 4. (a) MNZ, (b) ATZ, (c) BPA, (d) PE in the Si-O-C/PMS system. (e) The k_{obs} of MNZ, ATZ, BPA, PE degradation by different PMS dosage. Catalyst dosage: 0.1 g/L; PMS dosage: 0.5 mmol/L,1 mmol/L,2.0 mmol/L,3.3 mmol/L; Pollutant concentration: 10 mg/L.

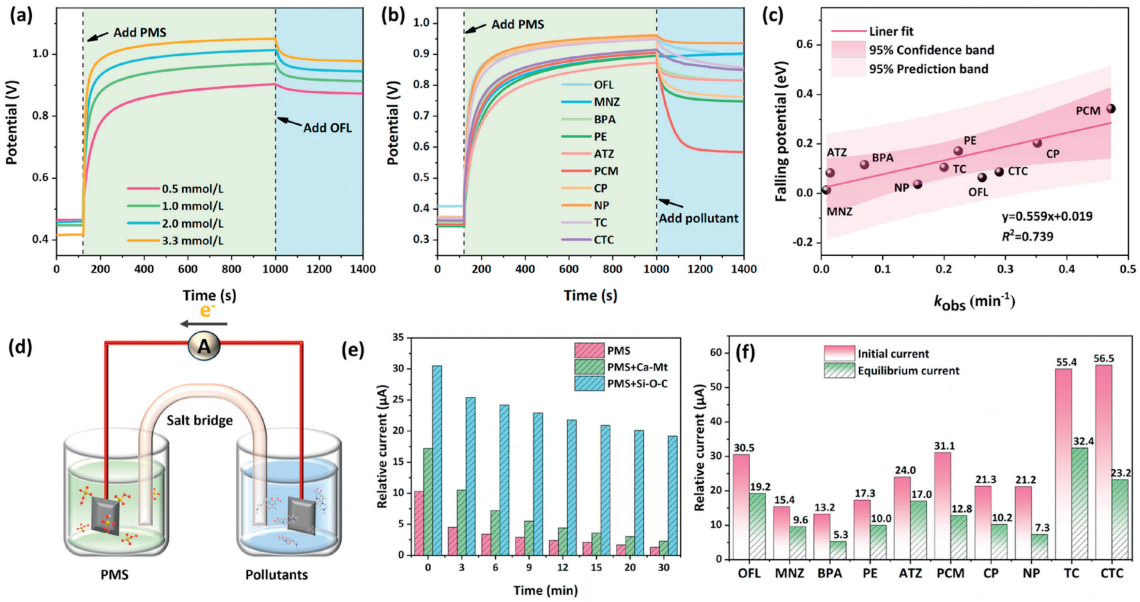


Fig. 5. Different falling potential trends after adding PMS dosage (a) and different pollutants (b). (c) Correlation between k_{obs} of different pollutants and their falling potentials obtained in the Si-O-C/PMS system. (d) A scheme of galvanic oxidation system. (e) Current generation in GOS coating with different catalysts (Ca-Mt and Si-O-C). (f) Current generation in GOS coating with different pollutants.

system. This observation aligns with the increased defect structures in the catalyst, emphasizing the enhanced interaction between PMS and Si-O-C, which accelerates the potential elevation [26]. The potential reduction noted at 1000 s after OFL addition in both Ca-Mt/PMS and Si-O-C/PMS systems is ascribed to electron chelation by organic pollutants [27], facilitating electron transfer from OFL to PMS *via* Si-O-C, thereby promoting PMS decomposition and OFL degradation. In stark contrast, the Ca-Mt/PMS system displayed minimal potential fluctuations, thereby highlighting the pronounced electron transfer dynamics specific to the Si-O-C/PMS system.

Significantly different potential changes were observed by adding different contaminants to the electrochemical Si-O-C /PMS system (Fig. 5b, Figs. S3 and S4 in Supporting information). The potential remained largely unchanged following the introduction of pollutants containing electron-withdrawing groups into the Si-O-C/PMS system such as MNZ and NP. The potential exhibited a significant decrease upon the introduction of pollutants containing electron-donating groups such as CP, PE, and PCM. The decrement in open-circuit potential subsequent to contaminant addition was indicative of the redox interaction between the contaminants and the Si-O-C/PMS* complex, culminating in the disintegration of surface complexes. Consequently, in the presence of contaminants, where PMS assumes the role of electron acceptor and contaminants act as electron donors, a variable electron transfer ensues, contingent upon the electron-donating capacity of the contaminants [28,29]. The linear correlation between the k_{obs} obtained in different contaminant systems and their decreasing potential was further confirmed by a correlation of $R^2 = 0.739$, as shown in Fig. 5c.

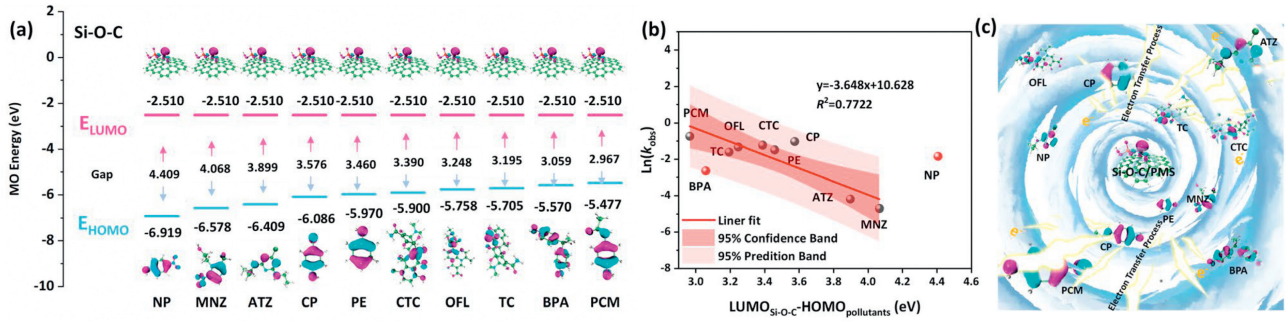


Fig. 6. (a) The LUMO (Si-O-C/PMS complexes) and HOMO pollutants. (b) The correction between the calculated gaps and lnk_{obs} data of pollutants. (c) Various organic pollutants degraded by Si-O-C/PMS *via* electron transfer process.

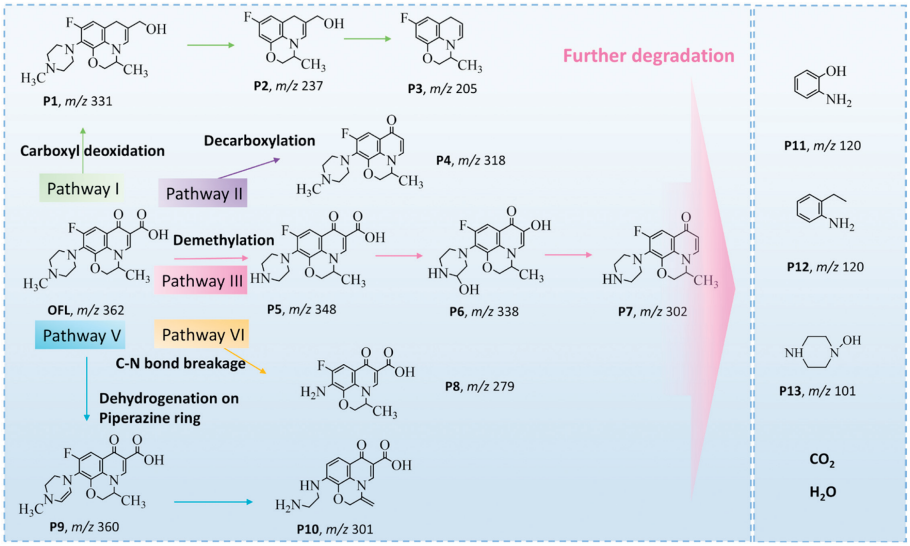


Fig. 7. Possible intermediates and proposed degradation pathways of OFL in Si-O-C/PMS system.

To eliminate other effects by splitting the PMS and contaminants into two half-cells (Fig. 5d), a galvanic oxidation system oxidation system (GOS) was developed to reveal the electron transfer process (ETP). If the electron transfer process (ETP) occurs in the Si-O-C/PMS system, the electrons could be transferred from the contaminant molecules to Si-O-C/PMS* through the electron channel. As shown in Fig. 5e and Fig. S5 (Supporting information), by adding OFL as a contaminant, the GOS system of Si-O-C showed a current of 30.5 μA, which was three times higher than that of bare graphite sheet electrodes, followed by Ca-Mt current of 17.2 μA, while the GOS of bare graphite sheet electrodes showed a lower current. This result further confirmed that Si-O-C greatly facilitated the electron transfer from OFL to PMS by forming stable complexes with PMS. In addition, the effects of different contaminants on the current changes were also determined in the Si-O-C based GOS system (Fig. 5f and Fig. S6 in Supporting information), in which CTC showed the highest current (56.5 μA). Thus, the electron-rich contaminants could trigger higher ETP by supplying more electrons from the contaminant molecules to the Si-O-C/PMS complex.

Analyzing the highest occupied molecular orbital (HOMO) and lowest unoccupied molecular orbital (LUMO) could enhance the understanding of ETP pathway for the degradation of versatile pollutants in Si-O-C/PMS system. The basis for the occurrence of ETP in the Si-O-C/PMS system was that electrons could transfer from the HOMO of the pollutants ($HOMO_{pollutants}$) to the LUMO of Si-O-C/PMS ($LUMO_{Si\text{-}O\text{-}C/PMS}$, −2.510 eV). As shown in Fig. 6a, the energy gaps between the $HOMO_{pollutants}$ and $LUMO_{Si\text{-}O\text{-}C/PMS}$ varied from 2.967 eV to 4.409 eV. Smaller energy gaps between $HOMO_{pollutants}$ and $LUMO_{Si\text{-}O\text{-}C/PMS}$ allowed more electrons to migrate from the pollutant molecule to the Si-O-C/PMS complex, resulting in the enhanced ETP oxidation towards the degradation of pollutants. Additionally, a strong linear correlation ($R^2 = 0.7722$) was found between the energy gap of $LUMO_{Si\text{-}O\text{-}C/PMS}$-$HOMO_{pollutant}$ and the ln(k_{obs}) (Fig. 6b). Notably, there were significant differences in the NP compared to the other pollutants, which may be due to the over-strong electron absorption properties of nitro. This further implied that pollutants having a smaller energy gap with the Si-O-C/PMS complex were more prone to be oxidized by the ETP at a higher rate (Fig. 6c).

The ultimate transformation of ofloxacin (OFL) within the Si-O-C/PMS system had been meticulously characterized (Fig. S7 in Supporting information). The delineation of its degradation pathways was presented in Fig. 7 and Table S3 (Supporting information). Five possible degradation pathways were proposed based on the detected degradation products by LC-MS. OFL could undergo oxidation immediately upon exposure to reactive radicals. In pathway I, deoxidation occurred on the carboxyl group, resulting in the formation of **P1** (*m/z* 331). The electron-donating characteristics of the electron-rich quinolone moiety make OFL vulnerable to radical attacks. In Pathway II, the decarboxylation occurred on the pyridine ring, which formed **P4** (*m/z* 318). In pathway III, demethylation occurred on the piperazine ring, resulting in the formation

of **P5** (*m/z* 348). In pathway IV, the C–N bond cleavage proceeded successfully, leading to the formation of **P8** (*m/z* 279). In pathway V, the dehydrogenation on the piperazine ring resulted in the production of **P9** (*m/z* 360). Subsequent reactions could cause ring openings on the piperazine ring, forming **P10** (*m/z* 301) and other possible low molecular weight substances.

In summary, we successfully synthesized two-dimensional montmorillonite-derived carbon materials with a Si-O-C structure by utilizing montmorillonite as the structural template. The catalyst exhibited remarkable efficiency as a PMS activator and facilitated effective catalytic degradation of various antibiotics through an electron transport process. The Si-O-C catalyst formed a complex with PMS on its surface, while pollutants acted as electron donors to the PMS complex *via* Si-O-C as a bridge, thereby achieving rapid pollutant degradation. These studies offer promising prospects for innovative preparation strategies of carbon catalysts and provide novel insights into antibiotic wastewater treatment. In future, novel reactor designs will be studied further to promote the practical application of this technology.

Declaration of competing interest

The authors declare that they have no known competing financial interests or personal relationships that could have appeared to influence the work reported in this paper.

CRediT authorship contribution statement

Wan-Yin Gao: Writing – original draft, Software, Methodology, Investigation, Data curation, Conceptualization. **Xiao-Qiang Cao:** Supervision, Funding acquisition. **Li-Fei Hou:** Data curation. **Hao-Yun Lu:** Data curation. **Zhao-Jing Zhu:** Resources. **Wen-Jia Kong:** Resources, Writing – review & editing. **Yang Zhang:** Writing – review & editing. **Yi-Zhen Zhang:** Writing – review & editing. **Ya-Nan Shang:** Writing – review & editing, Writing – original draft, Supervision, Funding acquisition, Conceptualization. **Xing Xu:** Writing – review & editing, Visualization, Conceptualization.

Acknowledgments

The research work was supported by National Natural Science Foundation of China (Nos. 52170086, 22476116, 52074176) and Natural Science Foundation of Shandong Province (Nos. ZR2021ME013, ZR2024ME156, ZR2022QB250). The authors also want to thank Conghua Qi from Shiyanjia Lab (www.shiyanjia.com).

Supplementary materials

Supplementary material associated with this article can be found, in the online version, at doi:10.1016/j.cclet.2025.111095.

References

[1] X. Liu, Z. Yang, H. Liu, et al., J. Hazard. Mater. 480 (2024) 136080.
[2] X. Yang, J. Qin, Z. Dai, et al., Prog. Nat. Sci. 33 (2023) 534–543.
[3] X. Yang, Q. Zhong, S. Liang, et al., Environ. Sci. Technol. 56 (2022) 5860–5873.
[4] K. Yujiao, Z. Ruxin, X. Xing, et al., Chin. Chem. Lett. 34 (2023) 108272.
[5] W. Wang, M. Chen, J. Colloid Inter. Sci. 613 (2022) 57–70.
[6] W. Tian, J. Lin, H. Zhang, et al., J. Hazard. Mater. 423 (2022) 127083.
[7] S. Yanan, K. Yujiao, X. Xing, Chin. Chem. Lett. 34 (2023) 108278.
[8] J. Wang, J. Li, Y. Li, et al., J. Materiomics 11 (2025) 100934.
[9] X. Wang, Z. Xiong, H. Shi, et al., Appl. Catal. B: Environ. 329 (2023) 122569.
[10] L. Wu, Z. Sun, Y. Zhen, et al., Environ. Sci. Technol. 55 (2021) 15400–15411.
[11] N. Li, R. Li, X. Duan, et al., Environ. Sci. Technol. 55 (2021) 16163–16174.
[12] X. Liu, X. Yan, W. Liu, et al., Sci. Bull. 68 (2023) 603–612.
[13] X. Xu, S. Wang, X. Duan, et al., Chin. Chem. Lett. 33 (2022) 663–673.
[14] X. Feng, C. Liu, R. Long, et al., Chem. Eng. J. 478 (2023) 147252.
[15] H.-Y. Zhu, M.T. Liu, G. Wang, et al., Rare Metals 43 (2024) 1686–1701.
[16] J. Zhang, Y. Ma, Y. Sun, et al., Chem. Eng. J. 471 (2023) 144837.
[17] J. Cao, S. Sun, X. Li, et al., Chem. Eng. J. 382 (2020) 122802.
[18] C. Chen, M. Yan, Y. Li, et al., Appl. Catal. B: Environ. 340 (2024) 123218.
[19] F. Xiao, Y. Wang, X… Xie, et al., Sep. Purif. Technol. 298 (2022) 121548.
[20] K. Yuan, C. Gao, G. Zhao, et al., Appl. Clay Sci. 249 (2024) 107260.
[21] X. Song, X. Zhou, X. Lv, J. Asian Earth Sci. 247 (2023) 105595.
[22] L.Z. Miao, Y.-X. Guo, Z.Y. Liu, et al., Chem. Eng. J. 467 (2023) 143451.
[23] K. Mi, X. Jiang, J. Yu, et al., J. Alloy. Compd. 933 (2023) 167851.
[24] Z. Hu, Q. Gong, J. Wang, et al., Nanomaterials 12 (2022) 2298.
[25] H. Zhong, Z. Gong, J. Yu, et al., Adv. Sci. 11 (2024) 2404958.
[26] X. Peng, J. Wu, Z. Zhao, et al., Chem. Eng. J. 429 (2022) 132245.
[27] J. Xie, L. Zhang, X. Luo, et al., Chem. Eng. J. 457 (2023) 141149.
[28] Z. Yang, H. Wang, Y. Li, et al., Chem. Eng. J. 499 (2024) 155810.
[29] X. Pan, S. Mei, W.J. Liu, et al., Chin. Chem. Lett. 34 (2023) 108034.